# Physico-Chemical and Mechanical Properties of Geopolymer/Zircon Composites

**Ljiljana Kljajević[1], Miloš Nenadović[2], Marijana Petković[2], Dušan Bučevac[1], Vladimir Pavlović[3], Nataša Mladenović Nikolić[4], Snežana Nenadović[1]**

[1]Department of Materials Science, "Vinča" Institute of Nuclear Sciences - National Institute of the Republic of Serbia, University of Belgrade, Belgrade, Serbia

[2]Department of Atomic Physics, "Vinča" Institute of Nuclear Sciences - National Institute of the Republic of Serbia, University of Belgrade, Belgrade, Serbia

[3]Institute of Technical Sciences of the Serbian Academy of Sciences and Arts, Knez Mihailova 35/IV, University of Belgrade, 11000 Belgrade, Serbia

[4]Department of Nuclear and Plasma Physics, "Vinča" Institute of Nuclear Sciences - National Institute of the Republic of Serbia, University of Belgrade, Belgrade, Serbia

**Abstract:**

The effect of zircon ($ZrSiO_4$) on the physico-chemical and mechanical properties of geopolymer/zircon composites was examined in this study. Four geopolymer/zircon composites containing 10, 20, 30 and 40 wt.% zircon were prepared from metakaolin with alkali activators. Characterization of the obtained geopolymers was performed by X-ray diffraction (XRD), Scanning electron microscope (SEM-EDS), Fourier transform infrared spectroscopy (FTIR) and Matrix-assisted laser desorption ionization time-of-flight mass spectrometry (MALDI-TOF). XRD results did not confirmed the formation of interconnected phases between added zircon, starting aluminum silicates and alkali activators. Compressive strength of prepared geopolymer was examined. The maximum obtained compressive strength of 70.15 MPa was measured in sample containing the smallest fraction of zircon, i.e., 10 wt.%. Addition of larger amount of zircon (20 wt.%) hinders the progress of geopolymerization reaction and consequently decreases compressive strength.

**Keywords**: Metakaolin; Zircon; Inorganic polymer; Compressive strength; MALDI-TOF.

## 1. Introduction

Zircon ($ZrSiO_4$) is known to be a good refractory material that is widely used in the steel industry. It shows excellent chemical stability and resistance to thermal shock owing to the very low coefficient of thermal expansion (~4.1 x $10^{-6}$/K) and low coefficient of thermal conductivity which was found to be 5.1 W/m$^o$C at room temperature and 3.5 W/m$^o$C at 1000$^o$C. In addition, high purity sintered zircon retains its bending strength up to temperature as high as 1400$^o$C [1-3]. These properties make zircon a promising structural ceramics for application where sudden temperature changes are expected. Zircon is tetragonal crystal which contains certain trace elements including mainly hafnium, phosphor, yttrium, uranium, and lanthanides [4,5]. It has been used for improving the mechanical and thermal properties of refractory materials owing to its good chemical stability and other favourable properties [6]. Geopolymers are ecological materials, which belong to a group of inorganic polymers, novel

_____

**\*) Corresponding author:** ljiljana@vin.bg.ac.rs

_____

civil engineering materials and filtering material for various pollutants [7,8]. From the ecological point of view, production of geopolymers, represents an environmentally friendly technology since it does not lead to the generation of additional amounts of carbon dioxide, which is a burden for the environment. In the late fifties Glukhovsky began the development of a new type of composite, through the process of consolidation of the activated precursors which he called "soil-cement" [9]. The versatility of the process allows its application not only to natural raw materials [10] but also to unconventional materials such as industrial and natural wastes [11]. The most recent scientific results highlight the alkali activation process as one of the possible routes towards the production of novel ceramic materials and cleaner production consolidated at low temperature [12-16]. The application and development of geopolymers as an alternative to the conventional cements is more intense due to a number of problems related to the cement industry and the tendency towards cleaner organic production. Cement industry has a major contribution to carbon dioxide ($CO_2$) emissions: one ton of cement produced, produces one ton of carbon dioxide [17,18].

Compared to cement composite materials, geopolymers have significantly better chemical resistance. Beside the fact that they do not react with aggressive ions from the environment, they are also resistant to sulphate corrosion, which ensures their durability and strength over a long period of time [8]. In addition to the potential application in the building [19-22], geopolymers can be used for many other purposes thanks to its properties and structural design. In this research an attempt to improve the mechanical properties of geopolymer/zircon composites by adding zircon mineral ($ZrSiO_4$) as inorganic additive was described.

The main goals of this paper are to study the effect of addition of zircon on the structural and mechanical properties of the geopolymer (GP) and to determine the role of $ZrSiO_4$ in the geopolymerization process. The properties of a geopolymer doped with various amounts of $ZrSiO_4$ were investigated. The special attention is devoted to the influence of zircon on compressive strength, which was considered as key material property for potential use in the civil engineering. Our previous investigations on the geopolymer [23,24] indicate that starting material has good properties for further modification in terms of improved mechanical properties.

## 2. Materials and Experimental Procedures
## 2.1. Preparation of geopolymer samples

Metakaolin (MK) was prepared by calcining kaolinite (Rudovci, Lazarevac, Serbia.) at 750°C in air. Heating rate was 10 °C/min whereas the soaking time at elevated temperature was 3 h. Commercially available zircon powder ($ZrSiO_4$, "Trebol", USA, ~ 40 μm) was used as the starting material for synthesis of geopolymer samples. Chemical analysis of the powder, given by the manufacturer, is as follows: $ZrO_2$ – 65 %, $SiO_2$ – 33 %, $Al_2O_3$ – 2 %, $TiO_2$ – 0.35 %, $Fe_2O_3$ – 0.05%. The alkaline solution was prepared from sodium silicate and and 12 M NaOH (volume ratio $Na_2SiO_3$/NaOH = 1.6).

The geopolymer (GP) samples were formed from metakaolin and zircon ($ZrSiO_4$). Prior to making geopolymer samples both zircon and metakaolin powder were ground. The weight fraction of $ZrSiO_4$ was in the range from 10 % to 40 % (Table I). Metakaolin and the alkaline solution (solid/liquid ratio was 0.9) were mixed for 10 min and then left at room temperature for 24 h. After that the mixture was kept at 50°C for additional 48 h in appropriate covered molds and subsequently aged at room temperature in controlled conditions for 28 days. Geopolymer samples are marked as $GPZr_{10}$, $GPZr_{20}$, $GPZr_{30}$, $GPZr_{40}$. The reference geopolymer sample was made by alkaline activation of metakaolin by alkaline activator contains 12 M NaOH solution ($GP_{Ref}$).

**Tab. I** Mixing design of the geopolymer and zircon.

| Samples | Metakaolin (wt.%) | Zircon (wt.%) |
|---|---|---|
| $GP_{Ref}$ | 100 | 0 |
| $GPZr_{10}$ | 90 | 10 |
| $GPZr_{20}$ | 80 | 20 |
| $GPZr_{30}$ | 70 | 30 |
| $GPZr_{40}$ | 60 | 40 |

## 2.2. Characterization of raw samples and geopolymer pasts

The phase composition of crushed samples was analyzed by X-ray diffractometry (XRD) using Ultima IV Rigaku diffractometer, equipped with Cu $K\alpha_{1,2}$ tube operated at 40 kV and 40 mA. The diffraction data were collected in $2\theta$ range from 5 to 80° using a scanning step size of 0.02° and scan rate of 10 °/min, for routine phase analysis. FTIR spectra were acquired at room temperature using Bomem (Hartmann & Braun) MB-100 spectrometer set to give undeformed spectra. The microstructure analysis was performed on Au-coated powdered samples using JEOL JSM 6390 LV electron microscope at 25 kV.

The obtained geopolymers were also characterized by Matrix-assisted laser desorption ionization time-of-flight mass spectrometry (MALDI-TOF). Since this method is not routinely applied for analyses of inorganic polymers, it was first necessary to test several matrices in order to acquire the best spectra and more information.

Samples were crushed mechanically and re-suspended in distilled water to give a concentration of approximately 1 mg/mL. A small volume of sample (0.5 µL) was applied on the stainless steel target plate, followed by the same volume of 2,5-dihydroxybenzoic acid (2,5-DHB) solution in methanol (0.5 mol/L). The mixture was then left at the room temperature to co-crystallize. MALDI TOF MS was performed at the Autoflex Speed device (Bruker, Bremen, Germany) equipped with pulsed smart beam [TM]-II laser emitting at 355 nm with a maximum frequency of 2 kHz. The spectra were acquired in the positive ion mode, with the linear detector at accelerating voltage -20 kV and in a delayed extraction conditions (delay time 100 ns). Each spectrum represents the average of 2000 individual laser shots at the repetition rate of 200 kHz.

The compressive strength of the tested samples was determined after 28 days air aging at room temperature. Test was performed on a HPN400 type press (ZRMK-Ljubljana).

## 3. Results and Discussion
## 3.1. XRD analysis

Fig. 1 shows XRD patterns of samples containing different fraction of zircon. The pattern of geopolymer powders exhibits a characteristic broad reflection hump between $2\theta=15°-33°$ which is assigned to amorphous phase [10]. It has been documented that the amorphous phase of aluminum silicates accelerates the process of geopolymerization [23]. The XRD pattern of $GP_{ref}$ sample confirmed the presence of following mineral phases: smectite, muscovite, illite, calcite and quartz. The quartz phase with characteristic peaks at $2\theta = 26.57°$ and 20.92° (ICSD 89279) was found to be the major phase. Furthermore, peak at $2\theta = 6.20°$ which may refer to smectite, appeared in the pattern. XRD patterns of samples containing different fractions of zircon exhibit characteristic peaks of zircon phase which are located at 20°, 26.96°, 35.71°, 43.77° and 53.56° of $2\theta$.
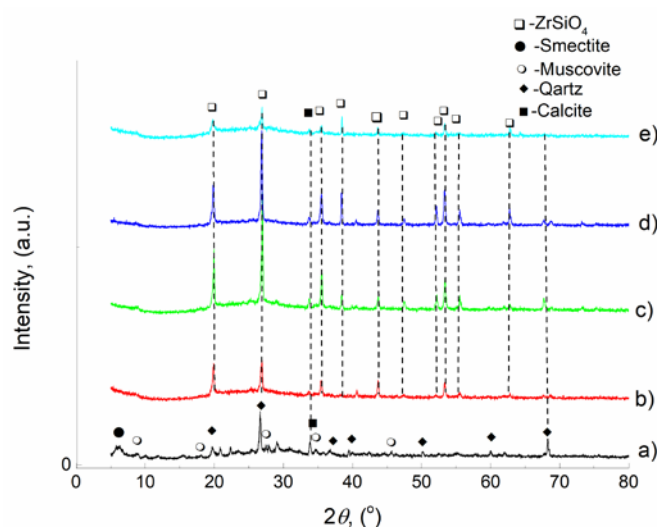
**Fig. 1.** XRD patterns of geopolimers containing different amount of zircon: a) 0 wt.% (GP_ref), b) 10 wt.% (GPZr_10), c) 20 wt.% (GPZr_20), d) 30 wt.% (GPZr_30) and e) 40 wt.% (GPZr_40).

## 3.2. FTIR analysis

FTIR spectra of all geopolymer samples (GPref and GPZr_10-GPZr_40) recorded between 400 and 4000 cm$^{-1}$ are shown in Fig. 2. Fig. 2a refers to a reference geopolymer sample. Also, with regard to all geopolymer composite with different zircon content (GPZr_10-GPZr_40), it can be concluded that there are no significant differences in the position and shape of the peaks.
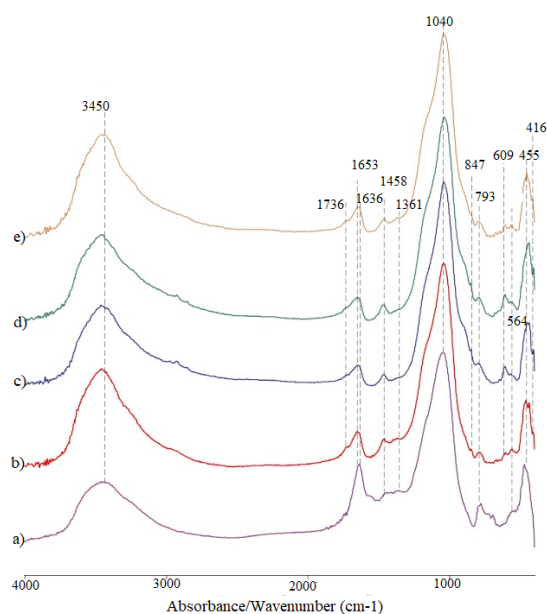


**Fig. 2.** FTIR spectra of geopolimers containing different fractions of zircon: a) 0 wt.% (GP_ref), b) 10 wt.% (GPZr_10), c) 20 wt.% (GPZr_20), d) 30 wt.% (GPZr_30) and e) 40 wt.% (GPZr_40).

The FTIR spectra of all geopolymers GPref and GPZr_10-GPZr_40 (Fig. 2b-Fig. 2e) show a broad band with a maximum at ~3450 cm$^{-1}$ and a sharp band at 1653 cm$^{-1}$. These bands are attributed to the stretching and deformation vibrations of the physically adsorbed

water molecules at the surface. The observed low OH stretching wave numbers suggest generally that hydrogen atoms of incorporated (OH)-groups are involved in hydrogen bonds to other, neighboring oxygen atoms. [23,25-29]. Although, all FTIR spectra show the occurrence the broad band in the range of 1010-1050 $cm^{-1}$ (at 1040 $cm^{-1}$) is due to symmetric stretching in random network with lower symmetry of Si-O-Si bond [21,30-32]. The samples, also, showed bands cantered at 1040 $cm^{-1}$ due to the asymmetric Si-O-Si stretching vibrations of transverse-optical ($TO_3$) mode and the longitudinal-optic ($LO_3$) part stretching vibrations, respectively [33,34,21]. Another band found at 1458 $cm^{-1}$ is arising due to $Na^+CO_3^{2-}$ vibration [32]. The band found at 1347-1370 $cm^{-1}$ (1361 $cm^{-1}$) arises due to 2vs, overtone of Al-O as Si cage ($TO_4$). Bands at 847 and 609 $cm^{-1}$ are assigned to Si-O-Zr stretching mode and Zr-O bond, respectively [35], while the band at 416 is assigned to Si-O bending bond [30,35]. The small band at 793 $cm^{-1}$ is ascribed to the vibration of tetrahedral unit containing Al-O bond [36]. The bands between of 2920-2931 $cm^{-1}$ assigned to symmetrical stretch of C-H mode of –$CH_2$-group [37-40].

Unlike $GPZr_{10}$-$GPZr_{40}$ samples, GPref sample does not show vibration bands at wave numbers 416, 609, 847 and 1736 $cm^{-1}$.

## 3.3. MALDI TOF analysis

Although not routinely used for characterization of geopolymers, MALDI TOF mass spectrometry was employed to analyze $GPZr_{10}$-$GPZr_{40}$ geopolimers, and identify the signals, which arise from geopolymer-derived ions. The main advantage of this method over other mass spectrometric methods typically used for geopolymer analyses is the possibility to analyze non-soluble compounds. Namely, the water suspension of geopolymer mixed previously with the matrix solution was applied on the MALDI target. Resulting co-crystals were homogenously distributed on the sample plate. The spectra were recorded due to the existence of spots with good matrix/analyte ratio. To acquire the spectra, which will reflect the composition of analyzed geopolymer, 2000 individual laser shots were applied all over the surface of a spot and resulting averaged spectra are presented. One should, however, keep in mind that the detected signals represent the ions obtained as a result of the laser ionization process, which are sufficiently stable to reach the detector. Signals are indicated according to their m/z position, whereas the signals, which arise from the matrix applied, are indicated by an asterisk. Each spectrum represents the average of 2000 individual laser shots, acquired at the laser frequency of 200 Hz.

Singly charged positive ions, which are generated from polymer molecules, are detected in the spectra presented in Fig. 3. Their number and variety increase with increasing weight fraction of $ZrSiO_4$ in GP, resulting in the spectrum which contains a large number of peaks at higher m/z ratios (>700) in the sample with the highest zircon fraction, i.e., $GPZr_{40}$ (Fig. 4). In other spectra, signals at m/z <700 are detected and they arise from the Al-Si-O, Zr-Si-O or Al-Si-O cluster with Zr, structure with varying ratio of different elements (cf. Table II for signal identity). The identity of ions at higher m/z ratios could not be resolved by MALDI TOF MS. According to Nazarenko et. al., 1979 [41] and Savin et. al., 1974 [42] such hydro complexes of zirconium as $Zr^{+4}$, $Zr(OH)^{+3}$, $Zr(OH)_2^{+2}$, $Zr(OH)_3^+$, $Zr(OH)_4$ exist in a solution under normal conditions, and they depend on the pH.

The absence of signals at higher m/z ratio in mass spectra given in Fig. 3, indicate that detected products are not results of reactions in the gas phase, but they are actual products of polymerization. Although without quantitative meaning, due to the insolubility of in acquired mass spectra confirm that $ZrSiO_4$ is involved in the polymerization process: signals detectable at higher masses in the spectrum of $GPZr_{40}$ (Fig. 4) imply that $ZrSiO_4$ stimulates the process of polymerization, even if its moiety does not increase with the increase of the amount of added $ZrSiO_4$, and the formation of a new bond, such as Zr-Al-Si-O was not evidenced.

_____
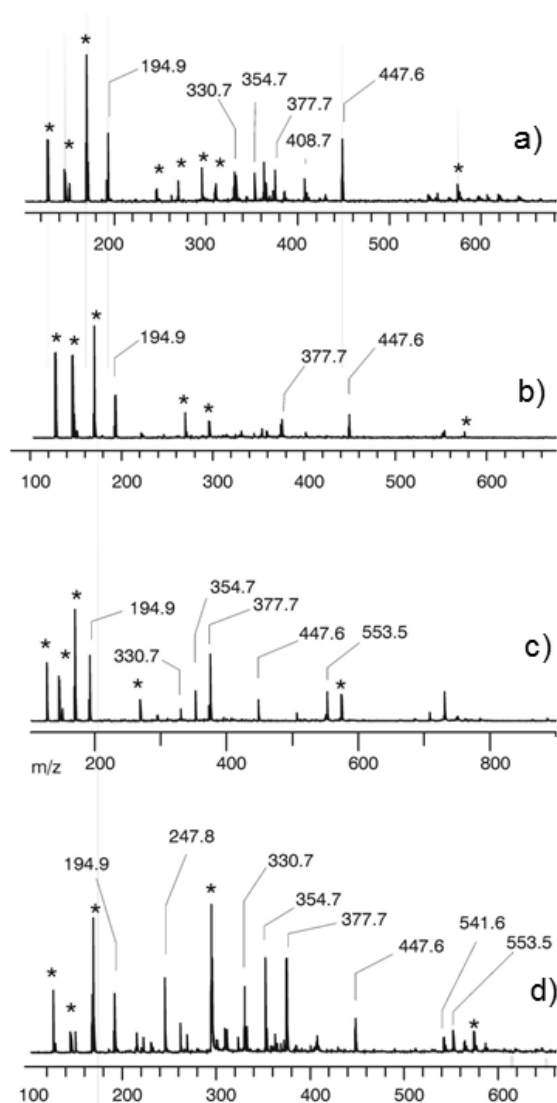


**Fig. 3.** Positive ion MALDI TOF mass spectra ofgeopolimers containing different fractions of zircon: a) 10 wt.% (GPZr$_{10}$), b) 20 wt.% (GPZr$_{20}$), c) 30 wt.% (GPZr$_{30}$) and d) 40 wt.% (GPZr$_{40}$).
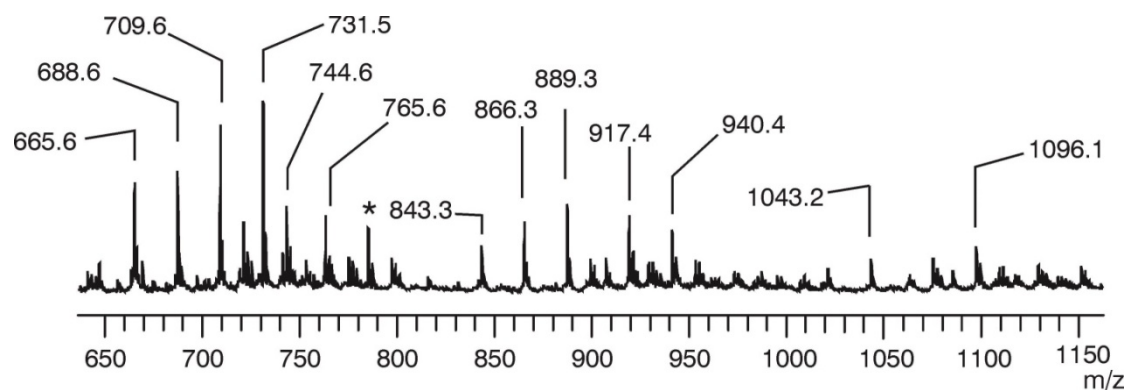


**Fig. 4.** High mass range of the positive ion MALDI TOF mass spectra ofsample containing 40 wt.% of zircon (GPZr$_{40}$).

_____

**Tab. II** The position (m/z) and the identity of signals detectable by the positive ion MALDI mass spectra of geopolymer/$ZrSiO_4$ composites.

| m/z | Identity |
|---|---|
| 194.9 | $AlSi_2O_7$ |
| 247.8 | $ZrSiO_8$ |
| 330.7 | $AlSiO_2$-$ZrSiO_4$-$Zr$ |
| 354.7 | $Zr_2.Si_2O_6$ +Na |
| 377.7 | $Si_2O_6$-$2Zr$+$2Na$ |
| 408.7 | $Al_2SiO_2$ -$ZrSiO_4$-$Zr$+$Na$ |
| 447.6 | $Al_2O_4$ $ZrSiO_4$-$2Zr$ |
| 541.6 | $Zr_3$-$Al_3Si_3O_5$+$Na$ |
| 553.5 | $Zr_3Al_3Si_3O_6$ +$Na$ |

## 3.4. SEM-EDS analysis

Fig. 5 depicts SEM/EDS images of reference geopolymer powder sample. This microstructure is important as a reference to be compared with the microstructure of prepared geopolymers containing zircon.
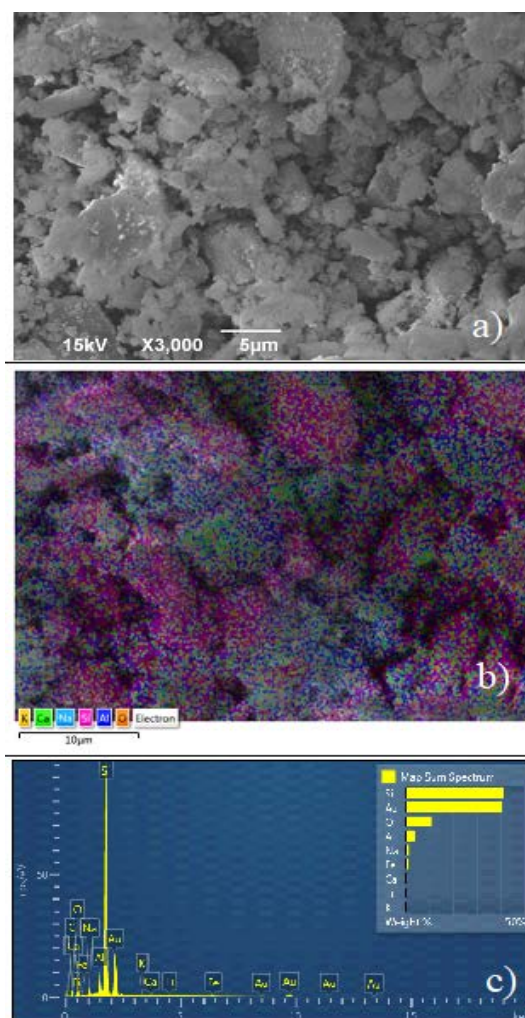


**Fig. 5.** SEM analysis of $GP_{ref}$: a) SEM micrograph, b) EDS mapping, c) EDS spectrum.

_____
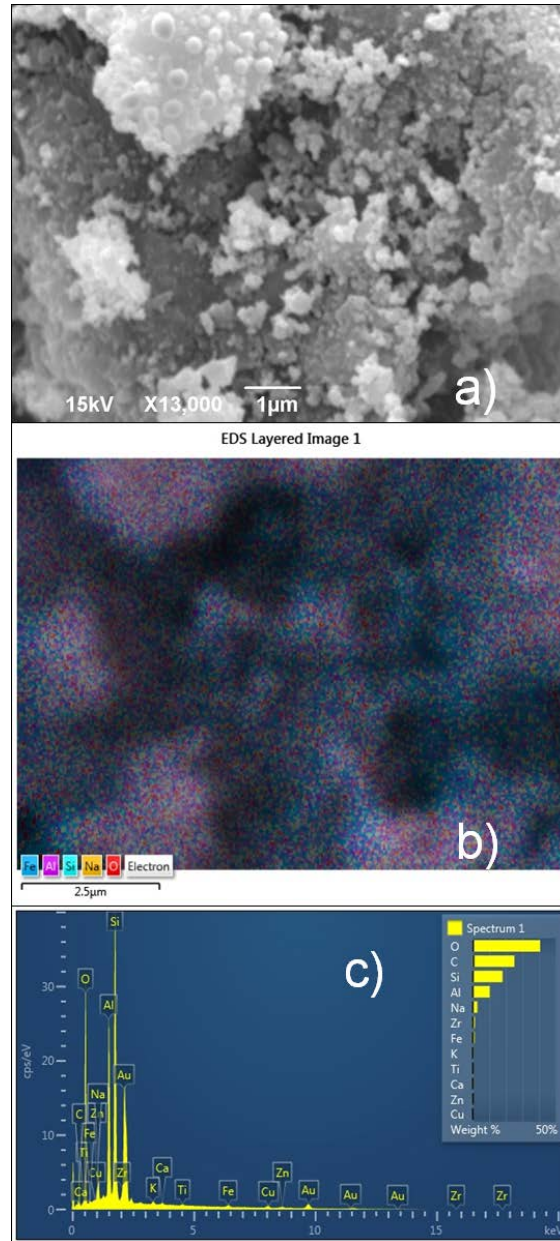


**Fig.6.** SEM analysis of GPZr$_{10}$: a) SEM micrograph, b) EDS mapping, c) EDS spectrum.

Fig. 6 shows SEM image and EDS analyses of synthesized GPZr$_{10}$ geopolymer. All geopolymer samples show amorphous gel microstructure, except a few particles showing spherical structure, produced from the water evaporation during curing process (aging time). These spherical features are dispersed on the surface and form porous microstructure. This is because the polymerization process starts from the surface of the reacting species. Faster polymerization leads to formation a gel structure of unreacted grains. Otherwise slower polymerization process increases the quantity of unreacted (spherical) features. EDS analysis of the investigated surface of the geopolymer sample GPZr$_{10}$, did not show the presence of Zr. The FTIR analysis (Fig. 2) confirmed that no direct peak assignment could be made to Si-O-Zr stretching modes. Also MALDI results confirmed the existence of Zr in the Zr1 sample with peaks found at 354.7 (Zr$_2$Si$_2$O$_6$ +Na), 377.7 (Si$_2$O$_6$-2Zr+2Na), 408.7 (Al$_2$SiO$_2$ -ZrSiO$_4$-Zr+Na), 477.6 (Al$_2$O$_4$ ZrSiO$_4$-2Zr).

The amorphous phase of raw materials determines the quantity of dissolved $SiO_2$ and $Al_2O_3$ and consequently the quantity obtained geopolymer gel. After addition of zircon material which looks like fine grains incorporated in the bulk matrix. Denser microstructure is obtained for the sample containing higher quantity of zircon ($GPZr_{20}$) which is presented in Fig. 7. The presence of $ZrSiO_4$ in the traces in sample $GPZr_{20}$ was confirmed. In addition to the SEM-EDS analysis, existence of $ZrSiO_4$ is also confirmed by FTIR and MALDI analyzes.
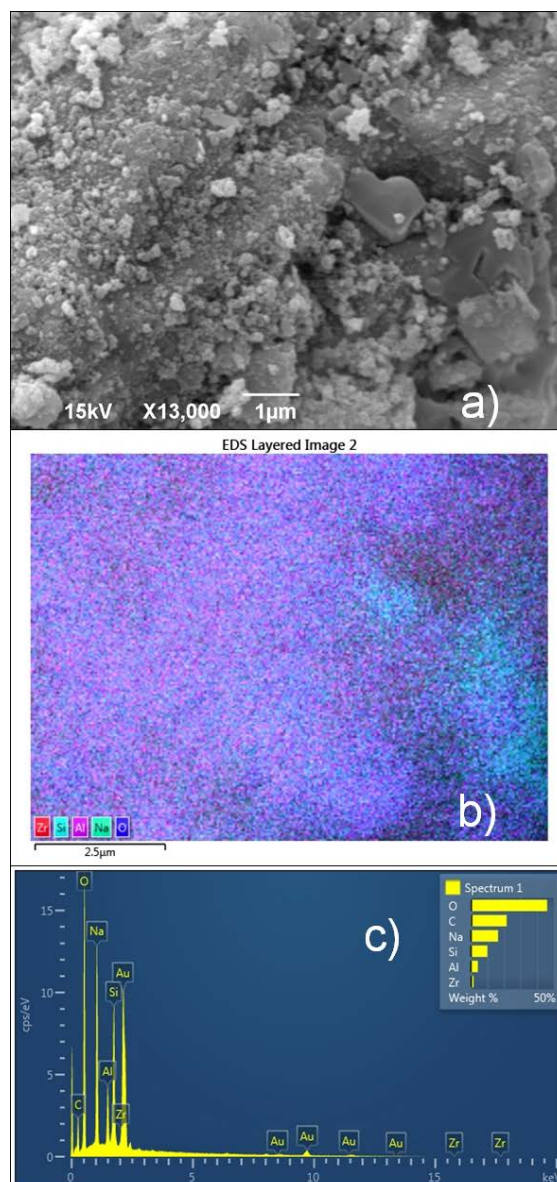
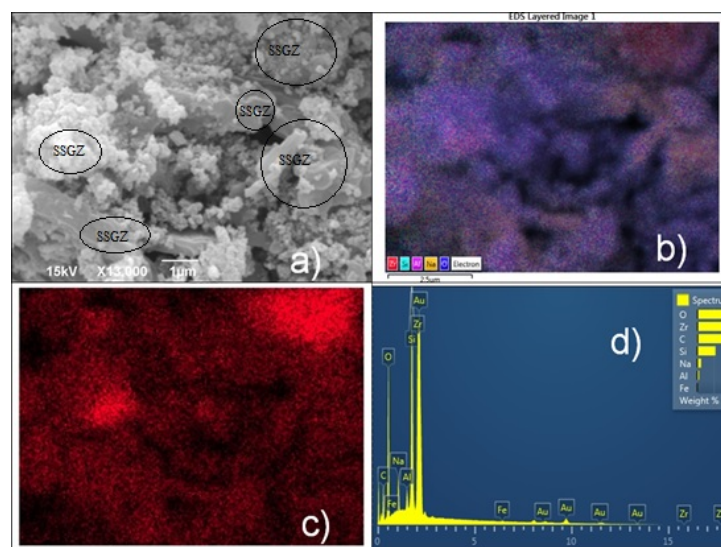

**Fig.7.** SEM analysis of $GPZr_{20}$: a) SEM micrograph, b) EDS mapping, c) EDS spectrum.

With an increase of the added zircon in metakaolin (Sample $GPZr_{30}$), a SEM-EDS analysis of the geopolymer matrix has also identified a higher percentage of $ZrSiO_4$ in the geopolymer, which can be seen from the SEM micrograph. Also, in Fig. 8, we find that the material is porous. MALDI results identify the peaks of newly formed structures with $ZrSiO_4$ in the alumino-silicate matrix. According to the sample mapping obtained Fig. 8b can be seen in one part of the sample accumulation of $ZrSiO_4$, while the distribution of the elements presenting the geopolymer matrix in the rest of the sample is fairly homogenous.

_____
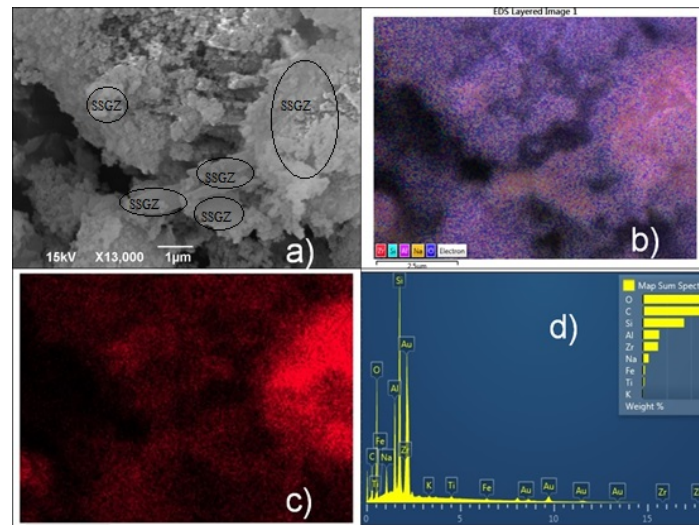


**Fig. 8.** SEM analysis of GPZr$_{30}$: a) SEM micrograph, b) and c) EDS mapping, d) EDS spectrum (SSGZ-Sodium silicate gel + Zircon is marked on the SEM images).

Fig. 9 shows the SEM-EDS images of the GPZr$_{40}$ sample. The SEM micrograph obtained by mapping the sample (Fig. 9b) shows more homogenous distribution of the present elements when compared to that of GPZr$_{30}$ sample. There is accumulation of ZrSiO$_4$ in one part of the sample, which indicates its uneven distribution over the entire volume of the sample. The SEM analysis (mapping) enabled a clearer insight into the distribution of the elements present in samples. Also, monitoring the porosity of the samples is much more efficient. MALDI analysis of the GPZr$_{40}$ sample revealed that during the geopolymerization there is an enhanced amount of ZrSiO$_4$ into the geopolymer matrix, with the intensities of the identified peaks associated with ZrSiO$_4$ being more pronounced. In the other words, with the increase in fraction of ZrSiO$_4$ to 40%, a larger amount of ZrSiO$_4$ could be incorporated in the geopolymer matrix causing formation of new structures, grouped separately from one another. In this way, as seen in SEM photographs, this is a quite porous material.



**Fig. 9.** SEM analysis of GPZr$_{40}$: a) SEM micrograph, b) and c) EDS mapping, d) EDS spectrum (SSGZ-Sodium silicate gel + Zircon is marked on the SEM images).

_____

### 3.5. Compressive strength of geopolymer/zircon composites

Fig. 10 shows the effect of zircon fraction on the compressive strength and bulk density of prepared geopolymer/zircon composites aged for 28 days at room temperature.
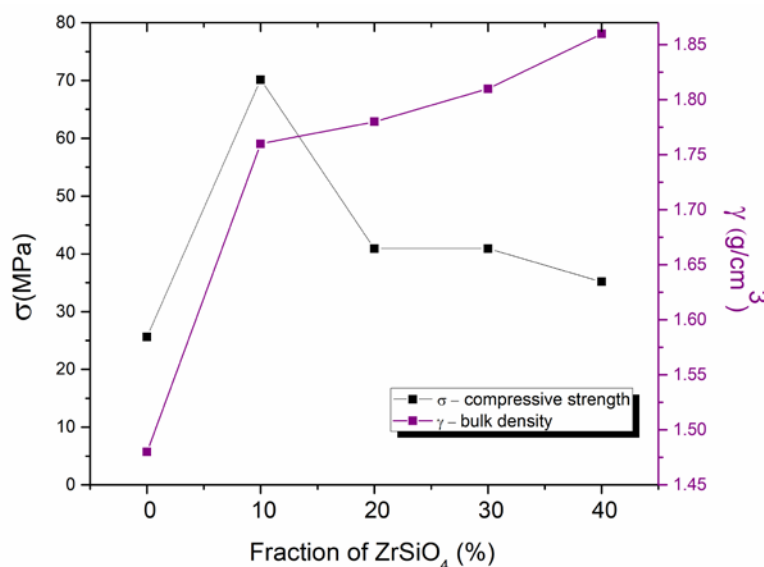


**Fig. 10.** The effect of zircon content on compressive strength and bulk density of geopolymer/zircon composite.

These fine particles of zircon lead to increased packing of formed geopolymer and consequently increase the density and decrease porosity. The obtained trend of porosity is opposite to that of compressive strength. Moreover, zircon might have an effective role in packing of polysialate structure produced from polymerization of metakaolin with alkali solution and forming a network which tends to increase the density and lower the porosity. The highest value of compression strength was measured in sample $GPZr_{10}$. The compression strength of samples containing 10 % zircon was three times higher than that of reference sample. The increased strength can be attributed to the presence of reinforcing zircon particles. However, further increase in the amount of zircon causes sharp decrease in strength caused by the interaction of tensile stress fields located around zircon particles. When hydration water is removed the structure of the geopolymer contracts and shrinks. However, the inert filler does not shrink and therefore tensions arise at filler-gel interfaces. At a certain point, when zircon particles are sufficiently close, the geopolymer matrix cannot compensate these tensions and the material cracks, either within the gel or at the $ZrSiO_4$-gel interface or both. Reduced strength of samples containing 20 wt.% (Fig. 10) indicates that the distance between zircon particles in these samples is short enough to cause interaction between stress fields around neighboring zircon particles and consequent material cracking. Further increase of zircon fraction does not case significant change in compression strength.

The gel-$ZrSiO_4$ tensions are higher with fine $ZrSiO_4$ filler because a greater surface area of the $ZrSiO_4$-gel interface is created. Censel, 2013 [43] show that the coarse size fraction was more effective at reducing the drying cracks than the medium or fine size fraction. Since $ZrSiO_4$ particles are 40 μm in size, this could be one of the reasons for the decrease in compressive strength with an increase in the proportion of $ZrSiO_4$ above 10 % compared to metakaolin as a precursor.

_____

## 4. Conclusion

One can conclude that the addition of specific amount of zircon ($ZrSiO_4$) improves compressive strength of metakaolin-based geopolymer. No new phases were formed upon the addition of zircon indicating that the zircon didn't participate in the geopolymerization reaction. In fact, zircon particles were embedded into polysialate network forming a rigid microstructure. The zircon content of 10 mas% which is added in metakaolin lead to the increase in compressive strength which reached maximum value of 70.1 MPa. Further increase in zircon content was followed by the decrease of compressive strength due to interaction of residual stresses around zircon particles. Therefore, $ZrSiO_4$, can be recommended as a material filler for materials demanding high density, but only up to 10 wt.% related to the metakaolin.

## Acknowledgments

## 5. References

1. Lj. Kljajević, A.Šaponjić, S. Ilić, S. Nenadović, M. Kokunešovski, A. Egelja, A. Devečerski, Ceram. Int. 42 (7) (2016) 8128.
2. Lj. Kljajević, S.Nenadović, M. Nenadović, D. Gautam, T. Volkov-Husović, A. Devečerski, B. Matović, Ceram. Int. 39 (5) (2013) 5467.
3. Lj. Kljajević, B. Matović, A. Radosavljević-Mihajlović, M: Rosić, S. Bošković, A. J. Alloys Compd. 509 (5) (2011) 2203.
4. Y. Kanno, J. Mater. Sci. 24 (7) (1989) 2415.
5. R. W. Hinton, B.G.J. Upton, Geochem. Cosmochim. Acta 55 (11) (1991) 3287.
6. M. F. Zawrah, Ceram. Int. 33 (5) (2007) 751.
7. J. Davidovits, Geopolymer, green chemistry and sustainable development, In Davidovits, J., (ed.) Proceedings of the world congress of Geopolymer, Institut of Geopolymer, St. Quentin, 2005, p.9-17.
8. F. Pacheco-Torgal, J. Castro-Gomes, S. Jalali, Constr. Build. Mater. 22 (2008) 1305.
9. V. D. Glukhovsky, Soil silicates. Gosstroyizdat, Kiev, 1959.
10. M. Ivanović, Lj. Kljajević, J. Gulicovski, M. Petković, I. Janković-Častvan, D. Bučevac, S. Nenadović, Sci. Sinter. 52 (2) (2020) 219.
11. S. Nenadović, G.Musci, Lj. Kljajević, M. Mirković, M. Nenadović, F. .Kristaly, I. Vukanac, Nucl. Technol. Radiat. Prot. 32 (3) (2017b) 261.
12. V. F. F. Barbosa, K. J. D. MacKenzie, Mater. Res. Bull. 38 (2003) 319.
13. S. Nenadović, Lj. Kljajević, S. Marković, M. Omerašević, U. Jovanović, V. Andrić, I. Vukanac, Sci. Sinter. 47 (2015a) 299.
14. Lj. Kljajević, Z. Melichova, D. Kisić, M. Nenadović, B. Todorović, V. Pavlović, S. Nenadović, Sci. Sinter. 51 (2) (2019a) 163.
15. Lj.M. Kljajević, Z. Melichova, M. D. Stojmenović, B. Ž. Todorović, V. B. Pavlović, N. M. Čitaković, S. S. Nenadović, Maced. J. Chem. Chem. Eng. 38 (2) (2019b) 283.
16. N. Mladenović, Lj. Kljajević, S. Nenadović, M. Ivanović, B. Čalija, J. Gulicovski, K. Trivunac, J. Inorg. Organomet. Polym. Mater. 30 (2) (2020) 554.
17. D. L. Y. Kong, J. G. Sanjayan, Cement Concrete Res. 30 (2008) 986.

_____

18. R. M. Novais, M. P. Seabra, J. A. Labrincha, J. Clean. Prod. 143 (2017) 1114.
19. Lj. Kljajević, S. Nenadović, M. Nenadović, N. Bundaleski, B. Todorović, V. Pavlović, Z. Rakočević, Ceram. Int. 43 (9) (2017) 6700.
20. I. V. Bošković, S. S. Nenadović, Lj. M. Kljajević, I. S. Vukanac, N. G. Stanković, J. M. .Luković, M. A. Vukčević, Nucl. Technol. Radiat. Prot. 33 (2) (2018) 188.
21. M. Ivanović, Lj. Kljajević, M. Nenadović, N. Bundaleski, I. Vukanac, B. Todorović, S. Nenadović, Mater. de Construccion 68 (330) (2018) e155.
22. S. S. Nenadović, C. Ferone, M. T. Nenadović, R. Cioffi, M. M. Mirković, I. S. Vukanac, Lj. M. Kljajević, J. Radioanal. Nucl. Chem. 325 (2020) 435.
23. S. A. Bernal, J. L. Provis, V. Rose, R. Mejía de Gutierrez, Cem. Concr. Compos. 33 (1) (2011) 46.
24. S. S. Nenadović, Lj. M. Kljajević, M. T. Nenadović, M. M. Mirković, S. B. Marković, Z. Lj. Rakočević, Environ. Earth Sci. 73 (2015b) 7669.
25. J. Chandradass, K. S. Han, and D. S. Bae, J. Mater. Process. Technol. 206 (2008) 315.
26. B. Saikia, G. Parthasarathy, J. Mod. Phys. 1 (4) (2010) 206.
27. B. Tyagi, K. B. Sidhpuria, B. Shaik, and R. V. Jasra, J. Porous Mater. 17 (2010) 699.
28. X. R. Chen, Y. H. Ju, and C. Y Mou, J. Phys. Chem. 111 (2017) 18731.
29. Y. Zhang, L. Pan, C. Gao, and Y. Zhao, J. Sol-Gel Sci. Technol., 58 (2911) 572.
30. E. S. Park, H. W. Ro, C. V. Nguyen, R. L. Jaffe, D. Y. Yoon, Chem. Mater., 20 (2008) 1548.
31. W. K. Part, M. Ramli, C. B. Cheah, Handb.: Low Carbon Concr. 77 (2016) 263.
32. W. K Part, M. Ramli, C. B. Cheah, Constr. Build. Mater. 77 (2015) 370.
33. H- Xu, J. S. J. Van Deventer, 15(12) (2002) 1131.
34. Z. Wang, Q. Xu, M. Xu, S. Wang and J. You, RSC Adv. 5 (2015) 11658.
35. P. Rovnaník, Constr. Build. Mater. 24 (7) (2010) 1176.
36. D. M. Pickup, G. Mountjoy, G. W. Wallidge, R. J. Newport, M. E. Smith, Phys. Chem. Chem. Phys. 1 (10) (1999) 2527.
37. P. F. McMillan, G. H Wolf., B. T. Poe, Chem. Geol. 96 (3-4) (1992) 351.
38. P. Innocenzi, J. Non Cryst. Solids, 316 (2–3) (2003) 309.
39. I. Jiménez-Morales, M. A. Río-Tejero Del, P. Braos-García, J. Santamaría-González, P. Maireles-Torres, A. Jiménez-López, Fuel Process. Technol. 97 (2012) 65.
40. R. R. Lloyd, J. L. Provis, J. S. J. van Deventer, J. Mater. Sci. 44 (2009) 620.
41. V. A. Nazarenko, V. P., Antonovich, E. M., Nevskaya, Metal ions hydrolysis in dilute solution, Atomizdat, Moscow, 1979, p. 101-103.
42. S. B. Savvin, V.P.Dedkova, D.O. Dzhashi, T.G. Akimova, E.M. Syanava, Zhurnal Analiticheskoj Khimii 34 (2) (1979) 300.
43. C. Kunzel,. Metakaolin based geopolymers to encapsulate nuclear water, PhD thesis, Imperial College London, London, 2013.

_____

**Сажетак:** *У овом раду је испитан утицај циркона (ZrSiO₄) на физичко-хемијске и механичке особине композита геополимер/циркон. Од метакаолина са алкалним активаторима припремљена су четири геополимер/циркон композита који садрже 10, 20, 30 и 40 теж.% циркона. Карактеризација добијених геополимера обављена је дифракцијом рендгенских зрака (XRD), скенирајућим електронским микроскопом (СЕМ-ЕДС), инфрацрвеном спектроскопијом Фуријеове трансформације (ФТИР) и ласерском десорпцијом потпомогнутом матриксом, јонизационом временском масеном спектрометријом (МАЛДИ-ТОФ). Резултати XRD нису потврдили формирање међусобно повезаних фаза између додатог циркона, почетних алуминијум силиката и алкалних активатора. Испитана је тлачна чврстоћа припремљеног геополимера. Максимална добијена чврстоћа на притисак од 70,15 MPa је измерена у узорку који садржи најмању фракцију циркона, односно 10 теж.%. Додатак веће*

_____

*количине циркона (20 теж.%) отежава ток реакције геополимеризације и самим тим смањује чврстоћу на притисак.*

**Кључне речи***: метакаолин, циркон, неоргански полимер, јачина притиска, МАЛДИ-ТОФ.*